6066 *Inorg. Chem.* **2010**, *49*, 6066–6076
DOI: 10.1021/ic100624q

Inorganic Chemistry
Article

Density Functional Theory Study of the Magnetic Circular Dichroism Spectra of Molybdenyl Complexes

Elizabeth Hernandez-Marin, Michael Seth, and Tom Ziegler*

Department of Chemistry, University of Calgary, Calgary, Alberta T2N 1N4, Canada

Received April 1, 2010

We report a density functional theory (DFT) study of the magnetic circular dichroism (MCD) spectra for four molybdenyl complexes: $[MoOCl_4]^-$, $[MoO(S_2C_2H_4)_2]^-$, [(Tp*)MoO(bdt)], and [(L3S)MoO(bdt)] (Tp* = hydrotris (3,5-dimethyl-1-pyrazolyl) borate; L3S = (2-dimethylethane-thiolate)bis(3,5-dimethylpyrazolyl)-methane; bdt =1,2-benzenedithiolate). The simulation of the temperature dependent MCD-bands (C-terms) that give rise to the spectra was performed using a method based on time-dependent DFT. In this method, the C-parameters are calculated by including spin−orbit perturbations. On the basis of the theoretical calculations, new or additional assignments are made for the MCD spectra of the complexes; specially for [(L3S)MoO(bdt)], for which case only tentative assignments of the excitations have been proposed in recent years.

Introduction

Molybdenyl ($[MoO]^{3+}$) complexes have been studied extensively to investigate the relation between molecular geometry, electronic structure, and reactivity of molybdenum complexes.[1−5] For the prototype complex $[MoOCl_4]^-$ there is a considerable body of both theoretical and experimental studies on the excitation energies,[6,7] and electron paramagnetic resonance (EPR) parameters.[8,9] About 30 years ago, it was found that enzymes like molybdenum hydroxylases appeared to facilitate oxo-transfer reactions.[10] Around the late 90's, the structures of the active site of various molybdoenzymes were determined via X-ray crystallography.[11−13] Since then, multiple efforts to create structural and functional analogues to the active site of the molybdoenzymes have been undertaken.[14−16] The active site of the mononuclear molybdoenzymes features an oxo group (Mo = O) binded to the metal and at least one pyranopterindithiolate entity. This molybdopterin cofactor closes a five-membered ene-1,2-dithiolate chelate ring.[14] Molecules which contain the molybdenyl species as well as one ([(Tp*)MoO(bdt)]) or two ($[MoO(S_2C_2H_4)_2]^-$) 1,2-dithiolate ligands have been synthesized and their structure determined.[17,18] Another molecule, [(L3S)MoO(bdt)], which in addition to the dithiolate (bdt) ligand contains a thiolate group coordinated to the molybdenum was recently prepared.[19]

Magnetic circular dichroism (MCD) and absorption spectroscopy are techniques that complement each other in studies on the electronic structure of molecules. MCD spectra, along with theoretical calculations, may be utilized to help in the assignment of excitations that are not easily discernible from the absorption spectrum. Recently it has become possible to simulate MCD spectra from first principles by the implementation of computer codes based on time-dependent density functional theory (TD-DFT)[20−23] or ab initio wave function methods.[24]

*To whom correspondence should be addressed. E-mail: ziegler@ucalgary.ca.

(1) Garner, C. D.; Hill, L. H.; Mabbs, F. E.; McFaden, D. L.; McPhail, A. T. *J. Chem. Soc., Dalton Trans.* **1977**, 853.
(2) Garner, C. D.; Kendrick, J.; Lambert, P.; Mabbs, F. E.; Hillier, I. H. *Inorg. Chem.* **1976**, *15*, 1287.
(3) Garner, C. D.; Hill, L. H.; Mabbs, F. E.; McFaden, D. L.; McPhail, A. T. *J. Chem. Soc., Dalton Trans.* **1977**, 1202.
(4) Garner, C. D.; Lambert, P.; Mabbs, F. E.; King, T. J. *J. Chem. Soc., Dalton Trans.* **1977**, 1191.
(5) Boorman, P. M.; Garner, C. D.; Mabbs, F. E. *J. Chem. Soc., Dalton Trans.* **1975**, 853.
(6) Nemykin, V. N.; Basu, P. *Inorg. Chem.* **2003**, 4046.
(7) Wang, F.; Ziegler, T. *Mol. Phys.* **2004**, *102*, 2585.
(8) Patchkovskii, S.; Ziegler, T. *J. Chem. Phys.* **1999**, *11*, 5730.
(9) Hadt, R. G.; Nemykin, V. N.; Olsen, J. G.; Basu, P. *Phys. Chem. Chem. Phys.* **2009**, *11*, 10377.
(10) Holm, R. *Chem. Rev.* **1987**, *87*, 251.
(11) Kisker, C.; Schindelin, H.; Pacheco, A.; Wehbi, W.; Garret, R.; Rajagopalan, K.; Enemark, J.; Rees, D. *Cell* **1997**, *91*, 973.
(12) Li, H.; Temple, C.; Rajagopalan, K.; Schindelin, H. *J. Am. Chem. Soc.* **2000**, *122*, 7673.
(13) McAlpine, A.; McEwan, A.; Bailey, S. *J. Mol. Biol.* **1998**, *275*, 613.
(14) Enemark, J. H.; Cooney, J. J. A.; Wang, J.-J.; Holm, H. R. *Chem. Rev.* **2004**, *104*, 1175.
(15) Sugimoto, H.; Suyama, K.; Sugimoto, K.; Miyake, H.; Takahashi, I.; Hirota, S.; Itoh, S. *Inorg. Chem.* **2008**, *47*, 10150.
(16) Sugimoto, H.; Tatemoto, S.; Suyama, K.; Miyake, H.; Itoh, S.; Dong, C.; Yang, J.; Kirk, M. L. *Inorg. Chem.* **2009**, *48*, 10581.
(17) Dhawan, I. K.; Enemark, J. H. *Inorg. Chem.* **1996**, *35*, 4873.
(18) Ellis, S. R.; Collison, D.; Garner, C. D.; Clegg, W. *J. Chem. Soc., Chem. Commun.* **1986**, 1483.
(19) Peariso, K.; Chohan, B. S.; Carrano, C. J.; Kirk, M. L. *Inorg. Chem.* **2003**, *42*, 6194.
(20) Seth, M.; Ziegler, T.; Banerjee, A.; Autschbach, J.; van Gisbergen, S.; Baerends, E. *J. Chem. Phys.* **2004**, *120*, 10942.
(21) Seth, M.; Ziegler, T. *J. Chem. Phys.* **2006**, *124*, 144105.
(22) Krykunov, M.; Seth, M.; Ziegler, T.; Autschbach, J. *J. Chem. Phys.* **2007**, *127*, 244102.
(23) Seth, M.; Ziegler, T.; Autschbach, J. *J. Chem. Phys.* **2008**, *129*, 104105.
(24) Ganyushin, D.; Neese, F. *J. Chem. Phys.* **2008**, *128*, 114117.

Published on Web 06/02/2010

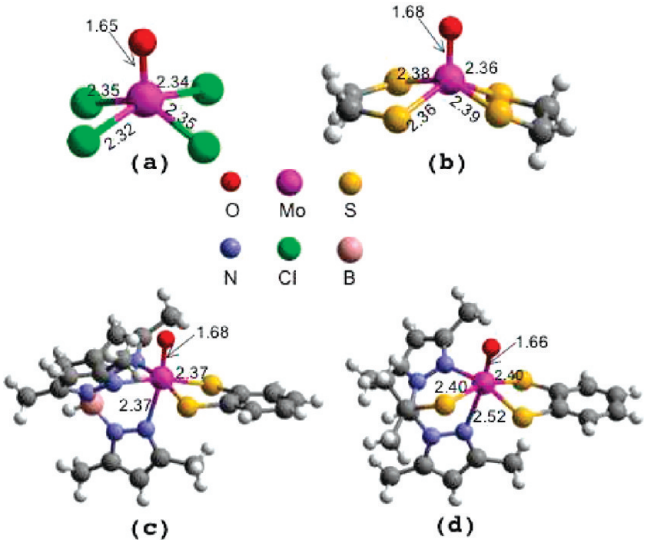

Figure 1. Molybdenyl complexes under investigation (a) $[MoOCl_4]^-$; (b) $[MoO(S_2C_2H_4)_2]^-$; (c) [(Tp*)MoO(bdt)]; (d) [(L3S)MoO(bdt)].

The objective of the present study is to carry out TD-DFT calculations on the MCD spectra of four molybdenyl complexes to further test the recent implementation within the ADF program[25] by simulating temperature dependent MCD bands (C-terms) and compare the results to experimental spectra. We shall also model the corresponding absorption spectra and provide an assignment aided by our MCD calculations. Our assignments will then be compared to those proposed previously. The four systems under investigation are (a) $[MoOCl_4]^-$, (b) $[MoO(S_2C_2H_4)_2]^-$, (c) [(Tp*)MoO(bdt)], and (d) [(L3S)MoO(bdt)], where Tp* = hydrotris (3,5-dimethyl-1-pyrazolyl) borate; L3S = (2-dimethylethanethiolate)bis(3,5-dimethylpyrazolyl)-methane; bdt = 1,2-benzenedithiolate.

Computational Methods and Details

Computational Parameters. All calculations were based on DFT as implemented in the ADF program version 2009 (www.scm.com). Use was made of the Becke−Perdew exchange-correlation functional (BP86)[26−28] and a standard triple-ζ STO basis with one set of polarization functions for all atoms. For the calculations, the 1s electrons of C, N, and O; the 1s2s2p electrons of S; and the 1s2s2p3s3p3d electrons of Mo were treated as frozen cores. The parameter for the precision of the numerical integration was set to 5.0. The simulated MCD spectra were based on the approach developed by Seth et al.[23] in which the C-parameters are calculated by including spin−orbit perturbations. This method makes use of time-dependent DFT (TD-DFT)[29] to describe the electronic excitations[7] and the zero-order regular approximation (ZORA) formalism to include relativistic effects.[30]

Computational Model Systems. Figure 1 displays the four systems under investigation: (a) $[MoOCl_4]^-$, (b) $[MoO(S_2C_2H_4)_2]^-$, (c) [(Tp*)MoO(bdt)], and (d) [(L3S)MoO(bdt)]. To calculate the excitation energies and MCD parameters, we use the experimental structures from the available crystallographic data[17−19,31] without any further optimization. For $[MoOCl_4]^-$ we also considered a "symmetrized experimental structure" in which we averaged the Mo−Cl distances and Cl−Mo−Cl angles to maintain C_{4v} symmetry. In this way we were able to gauge how distortions, as they occur for instance in crystals, influence the spectra.

Calculation of the MCD C-Parameters. MCD spectroscopy is based on the measurement of the difference in absorbance (ΔA) between left and right circularly polarized light traveling in the direction of a constant magnetic field B that is applied to the sample under study.

The MCD dispersion can be expressed as a function that is linear in the applied magnetic field strength B:[32]

$$\frac{\Delta A}{E} = \gamma B\left[A\left(-\frac{\partial f(E)}{\partial E}\right) + \left(B + \frac{C}{kT} f(E)\right)\right] \qquad (1)$$

where γ is a collection of constants, k is the Boltzmann constant and T, the temperature. E is the energy of the incident radiation and $f(E)$ is a band shape function. The constants A, B, and C are characteristic parameters specific to a given molecule and to a particular transition. It is customary to refer to the contributions in eq 1 containing A, B, and C as A-, B-, and C-terms, respectively. It has been pointed out that because the intensity of the C-terms is inversely proportional to the temperature, the temperature dependent C-terms dominate the MCD spectrum of paramagnetic systems.[33,34] and the B-terms may be neglected at low temperatures.[35] Therefore, our discussion of the MCD spectra is based on the description of the C-terms. We selected the band shape functions $f(E)$ to be Gaussians centered around the calculated excitation energy E_J

$$f_J = \frac{1}{\sqrt{\pi} W_J} e^{((E_J - E)/W_J)^2}$$

where the bandwidth parameters W_J are chosen to approximately reproduce the experimental MCD bands. In the implemented method, response theory is employed for the evaluation of the C-parameters and a detailed description of such calculations can be found elsewhere.[23] In general terms, the C_J parameter induced by the perturbation of the transition dipole for the excitation $A \rightarrow J$ in the γ direction by spin−orbit coupling can be written as:[23]

$$C_J \propto \sum_{\alpha\beta\gamma} \varepsilon_{\alpha\beta\gamma} \langle A|M^\alpha|J\rangle^{(1)\gamma} \langle J|M^\beta|A\rangle^{(0)} \qquad (2)$$

where $\varepsilon_{\alpha\beta\gamma}$ is the Levi-Civita symbol. Thus, if $\alpha\beta\gamma$ is a cyclic permutation of xyz, $\varepsilon_{\alpha\beta\gamma} = 1$. For other permutations $\varepsilon_{\alpha\beta\gamma} = -1$. When $\alpha = \beta$, $\alpha = \gamma$, or $\beta = \gamma$, then $\varepsilon_{\alpha\beta\gamma} = 0$. The operators M^α and M^β correspond to the Cartesian components for the electric dipole moment operator, A refers to the ground state, J to a given excited state, and the superscripts (1) and (0) refer to the first order spin−orbit perturbed and unperturbed integrals, respectively. Further, the term $\langle A|M^\alpha|J\rangle^{(1)\gamma}$ of eq 2 can be written formally as a sum-over-states expression:

$$\langle A|M^\alpha|J\rangle^{(1)\gamma} = \sum_{K\neq A} \langle K|M^\alpha|J\rangle^{(0)} \frac{\langle K|H_{SO}^\gamma|A\rangle^{(0)}}{E_K - E_A} + \sum_{K\neq J} \langle A|M^\alpha|K\rangle^{(0)} \frac{\langle J|H_{SO}^\gamma|K\rangle^{(0)}}{E_K - E_J} \qquad (3)$$

(25) Te Velde, G.; Bickelhaupt, F.; Baerends, E.; van Gisbergen, S.; Guerra, C.; Snijders, J.; Ziegler, T. *J. Comput. Chem.* **2001**, *22*, 931.
(26) Becke, A. *Phys. Rev. A:At., Mol., Opt. Phys.* **1998**, *38*, 3098.
(27) Perdew, J. *Phys. Rev. B* **1986**, *33*, 8822.
(28) Perdew, J. *Phys. Rev. B* **1986**, *34*, 7406.
(29) Casida, M. In *Advances in Density Functional Methods*; Chong, D. P., Ed.; World Scientific: Singapore, 1995; Vol. *1*, p 155.
(30) van Lenthe, E.; Baerends, J.; Snijders, J. *J. Chem. Phys.* **1993**, *99*, 4597.
(31) Blake, A. J.; Parsons, S.; Downs, A. J.; Limberg, C. *Acta Crystallogr.* **1995**, *C51*, 571.
(32) Stephens, P. *Annu. Rev. Phys. Chem.* **1974**, *25*, 201.
(33) Kirk, M.; Peariso, K. *Curr. Opin. Chem. Biol.* **2003**, *7*, 220.
(34) Lehnert, N.; DeBeer, S.; Solomon, E. I. *Curr. Opin. Chem. Biol.* **2001**, *5*, 176.
(35) Collocott, S. J.; Taylor, K. N. R. *J. Phys. C: Solid State Phys.* **1979**, *12*, 1767.

where H_{SO} is the spin−orbit operator. For qualitative analysis purposes, inspection of eqs 2 and 3 allows one to write a simplified expression for the C-parameter as:

$$C_J = C_J^G + C_J^E \quad (4)$$

where C_J^G represents the contribution due to the mixing of the ground state with excited states via spin orbit coupling and C_J^E represents the contribution due to the mixing of excited state J with other excited states.

We thus have

$$C_J^G = \sum_{\alpha\beta\gamma} \varepsilon_{\alpha\beta\gamma} \sum_{K\neq A} \langle K|M^\alpha|J\rangle^{(0)} \langle J|M^\beta|A\rangle^{(0)} \frac{\langle K|H_{SO}^\gamma|A\rangle^{(0)}}{E_K - E_A} \quad (5)$$

and

$$C_J^E = \sum_{\alpha\beta\gamma} \varepsilon_{\alpha\beta\gamma} \sum_{K\neq J} \langle A|M^\alpha|K\rangle^{(0)} \langle J|M^\beta|A\rangle^{(0)} \frac{\langle J|H_{SO}^\gamma|K\rangle^{(0)}}{E_K - E_J} \quad (6)$$

Results and Discussion

We shall now present the results from our calculations on the absorption and MCD spectra for each of the four systems considered in this study. First, we identify the transitions that give rise to the main absorption bands in the four simulated spectra. In some cases, weak excitations that are relevant for the MCD spectra are also mentioned. Next, the simulated MCD spectra are discussed in terms of their principal C_J-parameters. Further, the decomposition of the total value of the relevant C_J-parameters into C_J^G and C_J^E contributions will be tabulated. For the calculation of the C_J-parameter of excitation J, it is possible to quantify the contribution from the spin−orbit mixing of other states K with the primary state J. We shall do so when the contributions are dominated by one or two K-states. It also should be noted that several C-parameters might contribute to the same MCD band if the transitions associated with the different C-parameters are closely spaced.

Before continuing the discussion, some notes on the nomenclature used throughout the text: "C-parameter" refers to the calculated numerical value for a given excitation, while "C-term" or "MCD-term" is used to describe the different bands that make up the MCD spectrum. Further, C_J is the C-parameter due to excitation $A \rightarrow J$. The different C-terms in the experimental or simulated MCD spectra are indicated by the labels $C(E)_N$ for the bands on the experimental spectra, and $C(T)_N$ for the bands on the theoretical ones. N is a roman numeral. The molecular orbitals with dominating contributions from the ligands are named Lx (x = a,b,c,d; depending on the molybdenyl system under discussion), while the molecular orbitals where the major contribution originates from the metal d-orbitals are the Mo d_{ab} orbitals. Finally, we will follow the conventional expression "pseudo A-term" to describe two adjacent C-terms of opposite sign.

$[MoOCl_4]^-$. Although compounds that involve the $[MOX_4]^-$ anion (M = Cr, Mo, W; X = Cl, Br, SPh) are already well characterized structurally via X-ray crystallography,[3,36−38] there is still some disagreement with regard to the assignment of the electronic absorption spectra.

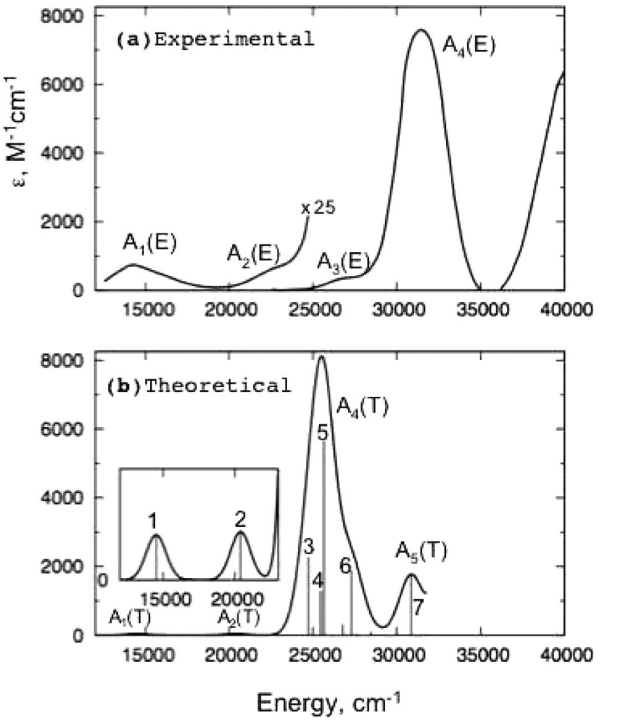

Figure 2. (a) Experimental[40] and (b) theoretical absorption spectra for $[MoOCl_4]^-$.

For example, in the case of the molybdenum system $[MoOCl_4]^-$, the excitation around 34000 cm^{-1} (Figure 2a) was tentatively assigned to a $d_{xy} \rightarrow d_{z^2}$ transition.[39] But in another study, it was assigned to a ligand-to-metal charge transfer (LMCT) transition.[40] The former assignment was suggested on the basis of earlier computational studies.[6,41] However, after the implementation of the unrestricted TD-DFT theory for doublet−doublet excitations it was found that a ligand to metal charge transfer transition fitted better to the high excitation energy at 34000 cm^{-1} whereas the $d_{xy} \rightarrow d_{z^2}$ transition was predicted to be at much lower energy.[7]

Figure 2 displays the experimental and the theoretical absorption spectra for $[MoOCl_4]^-$. The simulated absorption spectrum in Figure 2b corresponds to the unsymmetrical crystal structure of $[MoOCl_4]^-$. The excitation energies and oscillator strength values for the model with the X-ray coordinates are very similar to those of our symmetrized-C_{4v} model and to the energies from a previous unrestricted-TD-DFT study that used models optimized under C_{4v} symmetry.[7] Table 1 contains the corresponding excitation energies, oscillator strengths and assignments of the transitions labeled 1−7 on the calculated spectrum in Figure 2b. According to our calculations there are four distinct bands, with those at low energy (< 22000 cm^{-1}) being very weak. This is in agreement with the experimental results. The first experimental band $A_1(E)$ was assigned as a $d_{xy} \rightarrow d_{yz,xz}$ transition[39,40] and it corresponds to $A_1(T)$ of the simulated spectrum in Figure 2b. $A_1(T)$ is assigned to the $d_{xy} \rightarrow d_{yz,xz}$ transitions. Under the C_{4v} point group, the d_{yz} and

(36) Gahan, B.; Garner, C. D.; Hill, L. H.; Mabbs, F. E.; Hargrave, K. D.; McPhail, A. T. *J. Chem. Soc., Dalton Trans.* **1977**, 1726.
(37) Scane, J. G. *Acta Crystallogr.* **1967**, *23*, 85.
(38) Hill, L. H.; Howlader, N. C.; Mabbs, F. E.; McFadden, D. L.; McPhail, A. T. *J. Chem. Soc., Dalton Trans.* **1980**, 1475.
(39) Sabel, D. M.; Gewirth, A. A. *Inorg. Chem.* **1994**, *33*, 148.
(40) Carducci, M. D.; Brown, C.; Solomon, E. I.; Enemark, J. H. *J. Am. Chem. Soc.* **1994**, *116*, 11856.
(41) Deeth, R. *J. Chem. Soc., Dalton Trans.* **1991**, 1895.

Table 1. Theoretical Excitation Energies, Oscillator Strength (f), and Assignment of Excitations in Terms of Selected One-Electron Transitions for the Complex $[MoOCl_4]^-$

band $A_n(T)$	excitation	excitation energy[a]	transition[b]	%[c]	f
A_1	1	14510	α Mo d_{xy} →Mo d_{yz}	99.7	0.0002
A_2	2	20390	β La1 →Mo d_{xy}	98.6	0.0002
A_4	3	24720	β La2 →Mo d_{xy}	77.8	0.0103
	4	25470	α La1 →Mo d_{yz}	75.1	0.0058
	5	25660	β La3 →Mo d_{xy}	95.4	0.0254
	6	27310	β La5 →Mo d_{xy}	96.2	0.0085
A_4	7	30850	α La4 →Mo d_{yz}	82.0	0.0078

[a] Energies in cm^{-1}. [b] The orbitals are shown in Figure 3. [c] Percent contribution of the leading one-electron transition to the $A \rightarrow J$ excitation, where A represents the ground state.

d_{xz} orbitals are degenerate and constitute the 3e set in Figure 3.When the crystal structure is used, the slight distortion from the ideal C_{4v} symmetry causes the oscillator strength for the $d_{xy} \rightarrow d_{xz,yz}$ transitions to be small but nonzero with $f = 1.5 \times 10^{-6}$ a.u. for $d_{xy} \rightarrow d_{xz}$ and $f = 1.8 \times 10^{-3}$ a.u. for $d_{xy} \rightarrow d_{yz}$. On the basis of its polarization and vibrionic structure, the band $A_2(E)$ was previously assigned as a $d_{xy} \rightarrow d_{x^2-y^2}$ transition.[40] For the crystal structure, this excitation is calculated to occur at 22520 cm^{-1}. However, its oscillator strength is negligible (8.1×10^{-7} a.u.). Moreover, the $d_{xy} \rightarrow d_{x^2-y^2}$ transition is dipole forbidden under C_{4v} symmetry. In our calculations, the theoretical band $A_2(T)$ arises from the ligand to metal charge transfer (LMCT) La1→ d_{xy} (excitation 2, Table 1). The La1 orbital may be related to the a_2 irreducible representation and the SOMO d_{xy}, to b_2 (Figure 3). The $a_2 \rightarrow b_2$ transition is electric dipole forbidden, but since the crystallographic structure is slightly distorted, it is possible to obtain a weak intensity. In light of these results, it cannot be discarded that the $a_2 \rightarrow b_2$ LMCT may also contribute to the absorption band ($A_2(E)$) observed around 23000 cm^{-1}. Previously, the $a_2 \rightarrow b_2$ LMCT transition was assigned to an excitation observed at ~24000 cm^{-1} but only in the single crystal absorption spectrum of $[MoOCl_4(H_2O)]^-$. It was argued previously that such a transition could became allowed via spin−orbit coupling.[40]

The theoretical spectra fails to reproduce the experimental shoulder that corresponds to band $A_3(E)$ around 27000 cm^{-1}. This band was assigned as a $b_1 \rightarrow b_2$ transition[40] (La4 → Mo d_{xy}, according to Figure 3). This transition is symmetry forbidden in C_{4v}. Our calculations indicate that for the crystal structure, this excitation occurs at 25220 cm^{-1} with a very small oscillator strength (9.6×10^{-5} a.u.). Therefore, this excitation is not shown in Figure 2b. The strong band $A_4(T)$, which has its experimental counterpart in $A_4(E)$, is made up of several excitations, those labeled 3 to 6 were chosen for having a large oscillator strength. These excitations are all LMCT transitions. In line with the previous assignments,[39,40] excitations 3 and 5 are the La2 → d_{xy} and La3 → d_{xy} transitions, respectively. La2 and La3 belong to the 2e orbital set (Figure 3). In line with the previous assignment, excitation 6 is assigned to the La5 → d_{xy} transition, where the orbital La5 can be considered as one element of the degenerate out-of-plane Cl π 1e orbital set. The experimental excitation at 30000 cm^{-1} was assigned to the charge transfer transition from the out-of-plane Cl π orbitals of e symmetry to d_{xy}. One excitation that was not

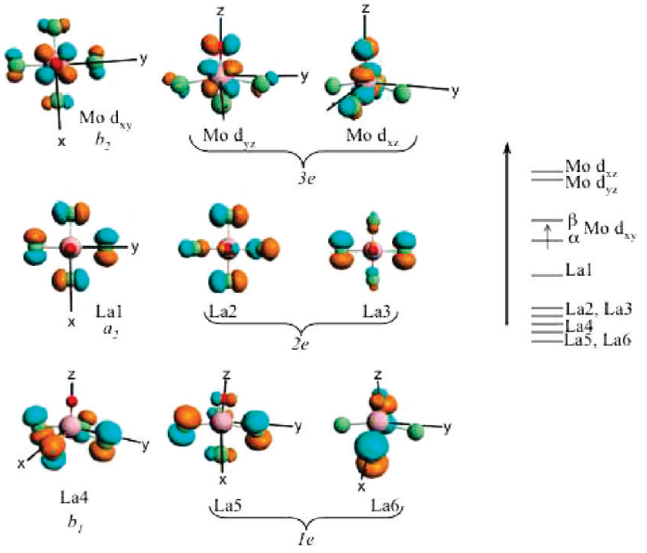

Figure 3. Plots of the molecular orbitals involved in the main transitions that give rise to the calculated electronic excitations for $[MoOCl_4]^-$. Also shown is a qualitative orbital energy level diagram.

previously assigned corresponds to the La1 → Mo d_{yz} transition. We calculated this transition at 25470 cm^{-1} (excitation 4 of medium-intensity, Table 1 and Figure 2). The equivalent transition, $a_2 \rightarrow$ 3e, for the C_{4v} model is calculated at 25520 cm^{-1}. The comparison of the experimental and calculated absorption spectra exhibits a reasonable qualitative agreement although the transition energies of the LMCT excitations were underestimated by approximately 0.7 eV (5500 cm^{-1}).

The MCD spectrum of $[Pr_4N][MoOCl_4]$ and $[PPh_4][MoOCl_4]$ has been recorded by Sabel and Gewirth,[39] as well as by Carducci et al.[40] Figure 4a displays the experimental spectrum for $[Pr_4N][MoOCl_4]$.[39] The low energy region of the spectrum reveals a pair of weak positive and negative MCD bands, $C_I(E)$ and $C_{II}(E)$ respectively, centered around 16000 cm^{-1}. They are followed by a sloping positive band ($C_{III}(E)$) that contains the previously assigned $d_{xy} \rightarrow d_{x^2-y^2}$ and $b_1 \rightarrow b_2$ transitions. The most intense band has the shape of a pseudo A-term, $C_{IV}(E)$, centered around 31000 cm^{-1}. Finally, a slightly weak negative band $C_V(E)$ was identified around 38000 cm^{-1}.

The theoretical MCD spectra for the crystal (dotted line) and symmetrized (broken line) structures are plotted in Figure 4b. The superposition of the symmetrized and distorted (crystal) structures is displayed in Figure 4 to make clear that both structures are very similar to each other. Nevertheless, the slight distortion is enough to create qualitative differences in the MCD spectra. The main difference between the spectra of the symmetrized and distorted (crystal) structures is found at low energies (inset of Figure 4b). For the C_{4v} system, the $d_{xy} \rightarrow d_{yz,xz}$ transition gives rise to a pseudo-A term feature around 15000 cm^{-1}. The pseudo-A term derivative shape signal appears because of the splitting of the degenerate e orbitals via spin−orbit coupling. However, it can be seen that the derivative signal is not symmetric. This is because the C-parameter due to the perturbation of the excited state by other excited states is calculated to be negative, thus decreasing the intensity of the positive end of the pseudo-A term. In the case of the distorted (crystal) structure, a

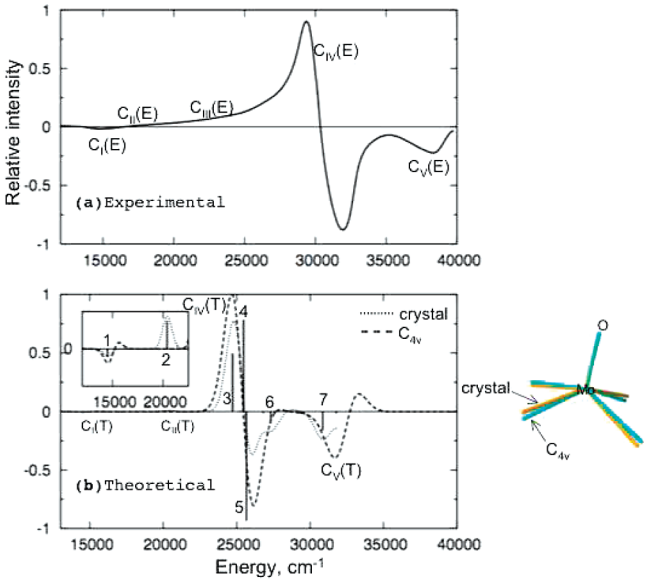

Figure 4. (a) Experimental (in poly(dimethylsiloxane) at 4.2 K and 6 T),[39] and (b) theoretical MCD spectra for $[MoOCl_4]^-$. Two theoretical spectra are plotted: one from the C_{4v} symmetrized structure (broken line); a second one from the crystal X-ray coordinates (dotted line). The most prominent individual C-parameters are shown with labels from 1 to 7. Also shown is the superposition of the symmetrized-C_{4v} and distorted (crystal) structures.

very weak negative band around 15000 cm^{-1} (band C_I, $d_{xy} \rightarrow d_{yz}$ transition) is calculated. For the crystal structure, the $d_{xy} \rightarrow d_{xz}$ transition gives a C-parameter 10 times less intense than the C-parameter for the $d_{xy} \rightarrow d_{yz}$ transition; thus, in practical terms it is not able to give rise to a visible C-term. The consequence is that the theoretical spectrum for the distorted (crystal) structure does not give rise to a pseudo-A term around 15000 cm^{-1}, in line with what one would expect on theoretical grounds from a unsymmetrical structure where the $d_{xy} \rightarrow d_{yz,xz}$ transitions are no longer degenerate.

Next, the positive band $C_{II}(T)$ at ~20000 cm^{-1} is due to the excitation 2 ($a_2 \rightarrow b_2$ transition, forbidden under C_{4v}, but not for the crystal structure). We are currently not able to account for the positive sloping C-term ($C_{III}(E)$) of the experimental spectra. It has been discussed already that the $b_1 \rightarrow b_2$ transition is symmetry forbidden and that such a transition is calculated to be zero even for the distorted (crystal) structure. Not surprisingly, the calculated C-parameter is also zero for the crystal structure.

A negative pseudo-A term centered on 25000 cm^{-1} is calculated for the symmetrized model. This pseudo-A term is made up itself by the superposition of 3 negative pseudo-A terms from the following transitions: $2e \rightarrow d_{xy}$ (excitations 3 and 5 for the crystal structure), $a_2 \rightarrow 3e$ (excitation 4, not considered in the experimental assignment), and $2e \rightarrow d_{xy}$ (excitation 6). The pseudo-A term due to the $2e \rightarrow d_{xy}$ transitions is calculated to be the dominant MCD term. For the crystal structure, although the band $C_{IV}(T)$ shows the alternation in sign, it is not quite obvious that it may constitute a pseudo-A term because the positive band is at least twice as intense as the negative one. However, the C-parameters at excitations 4 and 5 actually arise because of a pseudo-A mechanism. In this mechanism, for a contribution to C_J^E (e.g., $J = 4$ or 5) from excited state $K = 5$ or 4, respectively, there will be a contribution of the opposite sign to C_K^E from the excited state J. The same situation occurs with excitations 3 and 5. This is in line with the results from the symmetrized structure where the dominant term also arises from the $2e \rightarrow d_{xy}$ transition.

Table 2. Principal C-Parameters[a] from the Complex $[MoOCl_4]^-$

C-term	J^b	$C_J{}^c$	C_J^{Gd}	C_J^{Ee}
C_I	1	−0.09	0.29	−0.38
C_{II}	2	0.35	0.09	0.26
C_{IV}	3	24.45	1.76	22.69
	4	37.39	1.74	35.65
	5	−48.15	3.57	−51.72
	6	−4.70	1.38	−6.08
C_V	7	−7.68	0.01	−7.69

[a] Values in au × 10^{-3}. [b] See Table 1 for details on the excitations. [c] Total value of the C-parameter of excitation J. [d] Contribution due to the spin−orbit coupling perturbation of the ground state, eq 5. [e] Contribution from the perturbation of the excited state J, eq 6; for details, see eq 4.

The assignments that have created most controversy are the ones at higher energies, since they were originally assigned to a $d_{xy} \rightarrow d_{z^2}$ transition. It has been suggested that the assignment might be changed to a LMCT transition instead.[7] Considering that the experimental and calculated MCD spectra are in good qualitative agreement in the high-energy region, we thus provide an additional argument in favor of the LMCT assignment. The excitation at 38300 cm^{-1} was not explicitly assigned previously. For the crystal structure, we find that it may correspond to a b_1 (La4) $\rightarrow d_{yz}$ transition and that it gives rise to a negative C-term (band $C_V(T)$. See excitation 7 in Figure 4b), in line with the experimental observation. Moreover, the corresponding excitation for the C_{4v} symmetry is to a b_1 (La4) $\rightarrow$ 3e transition. This excitation generates a positive pseudo A-term. Therefore, the negative band $C_V(E)$ around 38000 cm^{-1} could be assigned to the negative portion of the pseudo A-term due to the transition from the out-of-plane Cl π to the metal $d_{yz,xz}$ orbitals. Finally, with respect to the origin of the C_J-parameters, Table 2 shows that the contribution C_J^E due to the spin−orbit perturbation of the excited state J is the leading term of the total C_J parameter. As it was already mentioned, it was generally not possible to identify a single excited state K that would account for the leading contribution to C_J^E. The only exception is, as expected, for the C_J parameters that generate pseudo-A terms, that is, $J = 3$, 4, and 5, as discussed earlier.

$[MoO(S_2C_2H_4)_2]^-$. Both the absorption and MCD spectra have been measured experimentally,[42] and the excitations of this complex were assigned mainly based on the MCD spectra aided by the use of a model idealized to C_{2v} symmetry and the application of the Slater transition state formalism[43] (ΔSCF DFT) to estimate the transition energies. The experimental and theoretical absorption spectra are presented in Figure 5. It has been pointed out that the approximations made in TD-DFT sometimes yield systematic errors in the calculated results.[44−46]

(42) McMaster, J.; Carducci, M. D.; Yang, Y.-S.; Solomon, E. I.; Enemark, J. H. *Inorg. Chem.* **2001**, *40*, 687.
(43) Slater, J. C. *Adv. Quantum Chem.* **1972**, *6*, 1.
(44) Jacquemin, D.; Perpète, E. A.; Ciofini, I.; Adamo, C. *Theor. Chem. Acc.* **2008**, *120*, 405.
(45) Le Guennic, B.; Hieringer, W.; Görling, A.; Autschbach, J. *J. Phys. Chem. A.* **2005**, *109*, 4836.

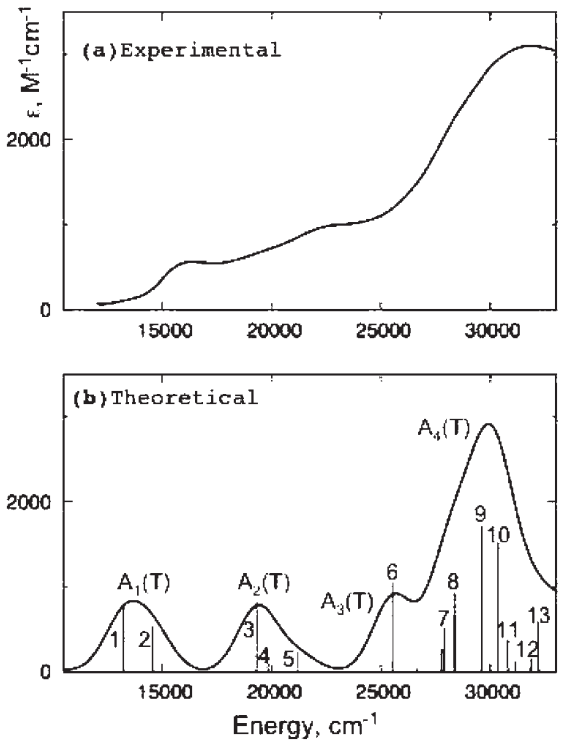

Figure 5. (a) Experimental (in dichloromethane solution at 298 K)[42] and (b) theoretical absorption spectra for $[MoO(S_2C_2H_4)_2]^-$. The theoretical excitation energies in (b) have been blue-shifted by 3000 cm^{-1} compared to the calculated values.

Thus, for a better quantitative comparison between the experimental and simulated spectra, a global blue-shift of 3000 cm^{-1} is applied to create the theoretical spectrum. The orbitals involved in the excitations are given in Figure 6 whereas the MCD spectra are displayed in Figure 7.

The first band in the experimental MCD spectrum is found at 11900 cm^{-1} ($C_I(E)$ of Figure 7a) with a corresponding weak feature in the experimental absorption spectrum at approximately 13400 cm^{-1} (Figure 5a). The positive term $C_I(E)$ corresponds to $C_I(T)$ of the simulated MCD spectrum (Figure 7b) and is assigned to the LMCT transition Lb3 →Mo d_{xy} (excitation 1 of Table 3) that in C_{2v} symmetry can be termed $b_1(\pi)$ → (Mo d_{xy}). The experimental weak feature at 13400 cm^{-1} as well as $C_I(E)$ were previously attributed to both the $b_1(\pi)$ →Mo d_{xy} and $b_2(\pi)$ →Mo d_{xy} transitions based on ΔSCF DFT calculations.[42] The first distinct band in the experimental absorption spectrum is found at 15 600 cm^{-1} and it corresponds to the positive $C_{II}(E)$ MCD term at 15 400 cm^{-1}. We attribute both features to the $b_2(\pi)$ → Mo d_{xy} transition (Lb4 →Mo d_{xy} excitation 2 of Table 3) which is responsible for the positive $C_{II}(T)$ term as well as (in conjunction with excitation 1) the simulated absorption band $A_1(T)$. It is likely that the energy separation between excitations 1 and 2 is underestimated in our calculations. In contrast, the $C_{II}(E)$ term has previously been assigned to the transitions $b_1(\sigma)$→Mo d_{xy} and $b_2(\sigma)$→Mo d_{xy}.[42] We find these transitions at higher energy as next discussed for the MCD-bands $C_{III}(T)$ and $C_V(T)$. The positive $C_{III}(E)$ term at 18800 cm^{-1} is ascribed to a $b_1(\sigma)$ →Mo d_{xy} transition (Lb5 →Mo d_{xy} excitation 3 of

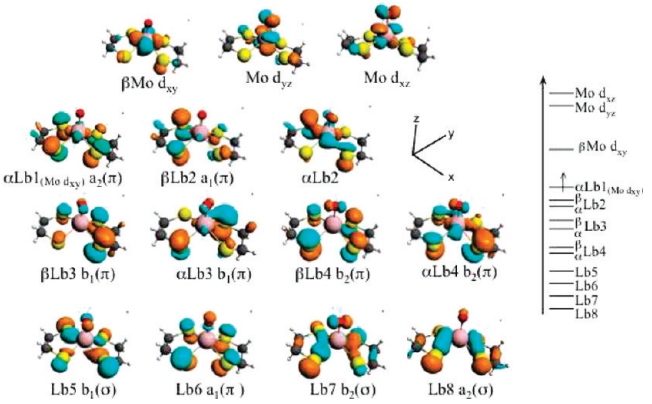

Figure 6. Plots of the molecular orbitals involved in the main transitions that give rise to the calculated electronic excitations for $[MoO(S_2C_2H_4)_2]^-$. Also shown is a qualitative orbital energy level diagram.

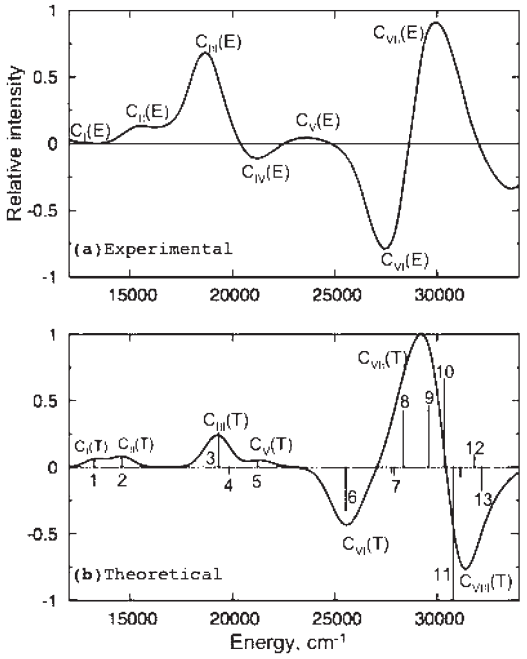

Figure 7. (a) Experimental (in 1,2-dichloroethane/DMF 1:1 frozen glass solution at 4.2 K and 5 T),[42] and (b) theoretical MCD spectra for $[MoO(S_2C_2H_4)_2]^-$. The excitation energies in (b) have been blue-shifted by 3000 cm^{-1} compared to the calculated values.

Table 3) which gives rise to the positive $C_{III}(T)$ term. The first negative C-term ($C_{IV}(E)$) in the experimental MCD spectrum appears at 21200 cm^{-1}. It seems at first glance not to have a counterpart in the simulated spectrum. However, transition 4 (Lb6 →Mo d_{xy} of Table 3) has a calculated negative C_4 parameter that is masked in $C_{III}(T)$ by transition 3, as it can be seen from Figure 7b. We suggest that $C_{IV}(E)$ should be designated to transition 4. This transition can be termed $a_1(\pi)$ →Mo d_{xy} in C_{2v} symmetry and should likely have been separated further from transition 3 so that it would not be masked by $C_{III}(T)$. The terms $C_{III}(E)$ and $C_{IV}(E)$ have previously been attributed to $a_1(\sigma)$→Mo d_{xy} and $b_{1,2}(\pi)$→Mo $d_{xz,yz}$, respectively.[42] The positive $C_V(E)$ term at 23500 cm^{-1} is attributed to transition 5 (Lb7 →Mo d_{xy} of Table 3) that is responsible for the positive $C_V(T)$ band. It can be described as $b_2(\sigma)$ →Mo d_{xy}. The $C_V(E)$ band has previously been associated with the $b_{1,2}(\pi)$ →Mo $d_{xz,yz}$ transitions.[42]

(46) Autschbach, J. *ChemPhysChem.* **2009**, *10*, 1757.

Table 3. Theoretical Excitation Energies, Oscillator Strength (f), and Assignment of Excitations in Terms of Selected One-Electron Transitions for the Complex $[MoO(S_2C_2H_4)_2]^-$

band $A_n(T)$	excitation	excitation energy[a,d]	transition[b]	%[c]	f
A1	1	13230	β Lb3 →Mo d_{xy}	93.3	0.0058
	2	14570	β Lb4 →Mo d_{xy}	93.1	0.0043
A2	3	19300	β Lb5 →Mo d_{xy}	98.8	0.0065
	4	19810	β Lb6 →Mo d_{xy}	98.8	0.0008
	5	21200	β Lb7 →Mo d_{xy}	99.1	0.0018
A3	6	25550	α Lb1 →Mo d_{xz}	95.5	0.0081
A4	7	27890	β Lb8 →Mo d_{xy}	78.3	0.0072
	8	28380	α Lb1 →Mo d_{yz}	96.7	0.0072
	9	29560	α Lb2 →Mo d_{xz}	38.4	0.0133
			β Lb2 →Mo d_{xz}	29.3	
	10	30360	α Lb3 →Mo d_{xz}	68.7	0.0118
	11	30800	β Lb2 →Mo d_{yz}	62.5	0.0030
	12	31840	α Lb2 →Mo d_{yz}	64.9	0.0014
	13	32180	α Lb4 →Mo d_{xz}	30.9	0.0045
			β Lb4 →Mo d_{xz}	26.6	

[a] Energies in cm^{-1}. [b] The orbitals are shown in Figure 6. [c] Percent contribution of the leading one-electron transition to the $A \rightarrow J$ excitation, where A represents the ground state. [d] The theoretical excitation energies have been blue-shifted by 3000 cm^{-1}.

The three terms $C_{III}(E)-C_V(E)$ are contained in the absorption around 20000 cm^{-1} as well as the low energy band of the visible spectrum at 23500 cm^{-1}. In the simulated absorption spectrum, transitions 3, 4, and 5 make up $A_2(E)$. It is likely that the energy spacing between the three transitions is underestimated in our calculations.

The dominant feature of the MCD spectrum for $[MoO(S_2C_2H_4)_2]^-$ is the pseudo A-band with a negative C-term ($C_{VI}(E)$) at 27600 cm^{-1} and a positive C-term ($C_{VII}(E)$) at 29900 cm^{-1}. We attribute $C_{VI}(E)$ to excitation 6 (Lb1 →Mo d_{xz}). Here, Lb1 is an $a_2(\pi)$ α-spin orbital with strong contributions from the sulfurs of the dithiolate ligands and a smaller contribution from the Mo d_{xy} atomic orbital (Figure 6). Thus excitation 6 is both a d-d transition and a LMCT, as it was already inferred.[42] The positive C-term $C_{VII}(E)$ at 29900 cm^{-1} contains excitations 8 ($a_2(\pi)$ →Mo d_{yz}), 9 ($a_1(\pi)$ →Mo d_{xz}), and 10 ($b_1(\pi)$) →Mo d_{xz}), all with significant positive C-parameters. Our assignments of $C_{VI}(E)$ and $C_{VII}(E)$ are essentially in line with those given previously.[42] Excitation 9, followed by excitation 10, have the strongest oscillator strength. They give rise to the dominant absorption band in the UV/vis spectrum at 31600 cm^{-1}. This is matched in the simulated spectrum by $A_4(T)$. The experimental spectrum shows the onset of a negative C-term at ~35000 cm^{-1} which is mirrored in the simulated MCD spectrum by $C_{VIII}(T)$. This feature is dominated by transition 11 ($a_1(\pi)$ →Mo d_{yz}). The remaining excitations 12 and 13 are assigned to $a_1(\pi)$ →Mo d_{yz} and $b_2(\pi)$ →Mo d_{xz} transitions, respectively.

In general the data in Table 4 indicates that C_J^E yields the largest contribution to the value of the C_J parameters, except for C_3. Moreover, the only case where the pseudo-A term mechanism plays a significant role on the origin of the C-parameters is for excitations 10 and 11. Once again, except for C_{10} and C_{11} it is not possible to single out a leading interaction with a specific excited state to account for the total value of the calculated C_J parameters.

[(Tp*)MoO(bdt)]. This complex of approximate C_s symmetry possesses a single dithiolene ligand, and it may be considered as a good starting approximation to the structure of the active site of molybdoenzymes. The first

Table 4. Principal C-Parameters[a] from the Complex $[MoO(S_2C_2H_4)_2]^-$

C-term	J[b]	C_J[c]	C_J^{Gd}[d]	C_J^{Ee}[e]
C_I	1	1.36	0.53	0.83
C_{II}	2	1.71	−0.93	2.64
C_{III}	3	5.09	7.72	−2.63
	4	−1.11	0.23	−1.34
C_V	5	0.95	−0.80	1.75
C_{VI}	6	−6.57	−0.07	−6.50
C_{VII}	8	8.41	−0.33	8.74
	9	9.01	0.15	8.86
	10	13.05	−0.26	13.31
C_{VIII}	11	−19.42	0.25	−19.67
	12	1.94	0.13	1.81
	13	−3.53	0.02	−3.55

[a] Values in au × 10^{-3}. [b] See Table 1 for details on the excitations. [c] Total value of the C-parameter of excitation J. [d] Contribution due to the spin−orbit coupling perturbation of the ground state, eq 5. [e] Contribution from the perturbation of the excited state J, eq 6; for details, see eq 4.

experimental C-term $C_I(E)$ appears in energy close to the first observed absorption band $A_1(E)$ at 9750 cm^{-1}. We associate $A_1(E)$ with the lowest calculated excitation $A_1(T)$ at 5820 cm^{-1} (1 of Figure 8b and Table 5). It corresponds to an Lc1 →Mo $d_{x^2-y^2}$ transition, where the "out-of-plane" orbital Lc1 may be related to the a′ irreducible representation of the C_s point group. It is consistent with this assignment that C_1 is calculated to be positive. The next MCD band $C_{II}(E)$ is negative and corresponds to the absorption $A_2(E)$ around 11000 cm^{-1}. We attribute it to the to the "out-of-plane" Lc2 (a″)→Mo $d_{x^2-y^2}$ transition which give rise to the negative C-term $C_{II}(T)$ and the weak absorption band $A_2(T)$ in our simulated spectra. We note that similar assignments for $A_1(E)$ and $A_2(E)$ have been given previously.[47,48]

The third absorption band $A_3(E)$ at 17,980 cm^{-1} has been characterized both as a d-d transition[48] as well as a "in-plane" a′ ligand to $d_{x^2-y^2}$ transition.[47] $A_3(E)$ is clearly related to the positive $C_{III}(E)$ term. We attribute it to the Lc4 →Mo $d_{x^2-y^2}$ transition $A_3(T)$ (excitation 3) which gives rise to the positive $C_{III}(E)$ term. Under C_s symmetry this transition may be regarded as an "in-plane" a″ →SOMO transition. The negative $C_{IV}(E)$ term at 20,000 cm^{-1} is well reproduced in the simulated MCD spectrum by $C_{IV}(T)$. According to our calculations $C_{IV}(T)$ draws contributions from the "in-plane" ligand to $d_{x^2-y^2}$ transitions 4, 5, and 6 as well as the d-d transitions 7 and 8. The $C_{IV}(E)$ term translates in the absorption spectrum to $A_4(E)$ which has its match in $A_4(T)$ of the simulated UV spectrum. The $A_4(E)$ band was previously assigned to an "in-plane" a′ →SOMO transition.[48]

The positive $C_V(E)$ band around 25,000 cm^{-1} is part of a pseudo A-term for which $C_{VI}(E)$ represents the negative part. A similar feature is apparent in the simulated MCD spectrum with the bands $C_V(T)$ and $C_{VI}(T)$. For $C_V(T)$ the contributing excitations are 9, 10, and 11 of Table 5. Here 9 is a "in-plane" Lc8 (a′) to Mo $d_{x^2-y^2}$ transition whereas 10 and 11 are excitations from the "out-of-plane" Lc2 (a″) orbital to d_{xz} and d_{yz}, respectively. The corresponding negative band $C_{VI}(T)$ is the result of the excitations 12, 13,

(47) Kirk, M.; Peariso, K. *Polyhedron* **2004**, *23*, 499.
(48) Inscore, F. E.; McNaughton, R.; Westcott, B. L.; Helton, M. E.; Jones, R.; Dhawan, I. K.; Enemark, J. H.; Kirk, M. L. *Inorg. Chem.* **1999**, *38*, 1401.

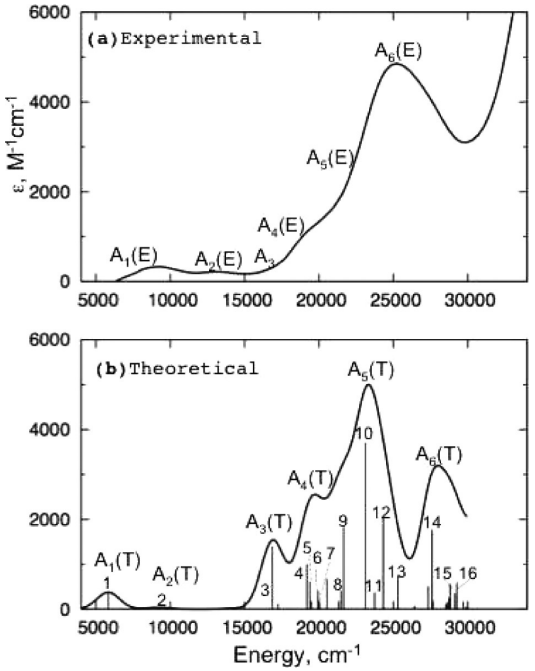

Figure 8. (a) Experimental (in 1,2-dichloroethane solution at room temperature)[47] and (b) theoretical absorption spectra for [(Tp*)MoO(bdt)].

Table 5. Theoretical Excitation Energies, Oscillator Strength (f), and Assignment of Excitations in Terms of Selected One-Electron Transitions for the Complex [(Tp*)MoO(bdt)]

band $A_n(T)$	excitation	excitation energy[a]	transition[b]	%[c]	f
A_1	1	5820	β Lc1 →Mo $d_{x^2-y^2}$	99.6	0.0049
A_2	2	9200	β Lc2 →Mo $d_{x^2-y^2}$	99.7	0.0005
A_3	3	16900	β Lc4 →Mo $d_{x^2-y^2}$	97.4	0.0182
A_4	4	19190	β Lc5 →Mo $d_{x^2-y^2}$	80.2	0.0130
	5	19390	β Lc6 →Mo $d_{x^2-y^2}$	77.0	0.0080
	6	19920	β Lc7 →Mo $d_{x^2-y^2}$	83.4	0.0055
	7	20040	α Mo $d_{x^2-y^2}$ →Mo d_{xz}	67.1	0.0164
A_5	8	21490	α Mo $d_{x^2-y^2}$ →Mo d_{yz}	51.2	0.0054
	9	21660	β Lc8 →Mo $d_{x^2-y^2}$	91.7	0.0236
	10	23130	β Lc2 →Mo d_{xz}	50.6	0.0480
	11	23740	β Lc2 →Mo d_{yz}	85.3	0.0265
	12	24330	β Lc9 →Mo $d_{x^2-y^2}$	80.7	0.0265
	13	25320	α Lc3 →Mo d_{xz}	86.2	0.0095
A_6	14	27610	β Lc3 →Mo d_{xz}	78.3	0.0229
	15	29130	β Lc4 →Mo d_{xz}	56.7	0.0046
	16	29260	β Lc4 →Mo d_{xz}	30.9	0.0076

[a] Energies in cm^{-1}. [b] The orbitals are shown in Figure 10. [c] Per cent contribution of the leading one-electron transition to the $A \rightarrow J$ excitation, where A represents the ground state.

and 14. Here 12 is an "out-of-plane" Lc9 (a′) to Mo $d_{x^2-y^2}$ transition whereas 13 and 14 constitute excitations from Lc3 to d_{xz}. Here Lc3 contains contributions mainly from the axial pyrazolyl ring. Excitation 10 is very intense and responsible for the strong absorption band $A_6(E)$ which also have contributions from 11 and 12. On the other hand, $A_5(E)$ arises according to our calculations from 9 with a considerable oscillatory strength. An earlier theoretical study assigned $A_5(E)$ to "out-of-plane" (a″) to d_{xz},d_{yz} transitions whereas $A_6(E)$ was attributed to "out-of-plane" ligand (a′) to d_{xz}, d_{yz} transitions.[48] We finally have at highest energy on both the experimental and simulated MCD spectrum a positive C-term $C_{VII}(T)/C_{VII}(E)$. We find that $C_{VII}(E)$ stems from the excitations 15 and 16 because of "in-plane" Lc4 (a″) transitions to Mo d_{xz}.

Table 6. Principal C-Parameters[a] from the Complex [(Tp*)MoO(bdt)]

C-term	J[b]	C_J[c]	C_J^{Gd}[d]	C_J^{Ee}[e]
C_I	1	0.70	1.06	−0.36
C_{II}	2	−1.02	−0.85	−0.17
C_{III}	3	4.87	6.54	−1.67
C_{IV}	4	5.56	−3.46	9.02
	5	−6.44	−1.77	−4.67
	6	−11.34	−2.16	−9.18
	7	4.94	1.47	3.47
	8	−9.83	−1.68	−8.15
C_V	9	7.83	6.29	1.54
	10	35.93	1.11	34.82
	11	−15.93	1.13	−17.06
C_{VI}	12	−7.14	−5.39	−1.75
	13	−5.22	−0.89	−4.33
	14	1.25	−0.44	1.69
C_{VII}	15	9.49	−0.03	9.52
	16	8.05	−0.12	8.17

[a] Values in au × 10^{-3}. [b] See Table 1 for details on the excitations. [c] Total value of the C-parameter of excitation J. [d] Contribution due to the spin−orbit coupling perturbation of the ground state, eq 5. [e] Contribution from the perturbation of the excited state J, eq 6; for details, see eq 4.

Table 6 shows that, except for the excitations 3 and 9, the total value of the C-parameters is dominated by the spin−orbit coupling of the excited states. For excitations 3 and 9, the C_J^G term that arises from the spin−orbit perturbation of the ground state represents the major contribution to the total value of the C-parameter. Some pairs of states like (4,5) and (10,11) are coupled strongly by spin−orbit coupling. We get as a result within each pair C-parameters of opposite signs, Figure 9 and Table 6.

[(L3S)MoO(bdt)]. This complex represents a model compound that closely approximates the active site structure of the reduced forms of the molybdoenzyme sulfite oxidase because in addition to the dithiolate ligand, there is an extra equatorial thiolate ligand coordinated to the molybdenum (Figure 1d). The absorption and MCD spectra for this complex have been measured recently,[47] and their respective experimental and calculated spectra are shown in Figures 11 and 12. The 9750 cm^{-1} band was suggested to be a LMCT originating from some out-of-plane dithiolate ligand orbital to the SOMO. Likewise, the excitation at 17980 cm^{-1} was tentatively assigned as the in-plane a′ → SOMO transition. However, no definite assignments were proposed.[47] The good agreement between the experimental and calculated absorption spectra is clear from Figure 11. Table 7 lists the main transitions that give rise to the six distinct bands that appear on the calculated spectrum shown in Figure 11b. We assign the weak excitation at 9400 cm^{-1} as an "out-of-plane" Ld2 a″ → Mo d_{xy} (SOMO). Note that here we have used the same nomenclature as for the previous complex [(Tp*)MoO(bdt)]. This is possible because the orbitals Lc2 (Figure 10) and Ld2 (Figure 12) are essentially similar. A stronger excitation 2 appears approximately at 14000 cm^{-1} and is assigned to the Ld3 →Mo d_{xy} transition. Notably, the Ld3 orbital has a considerable contribution from the S p_z orbital on the thiolate. At 15400 cm^{-1} (excitation 3), there is a weak Ld4 →Mo d_{xy} transition where the molecular orbital Ld4 contains major contributions from "in-plane" p-orbitals of both the thiolate and the dithiolate. Excitation 4 at 19460 cm^{-1} is assigned as an "out-of-plane" Ld1 →Mo d_{yz} transition.

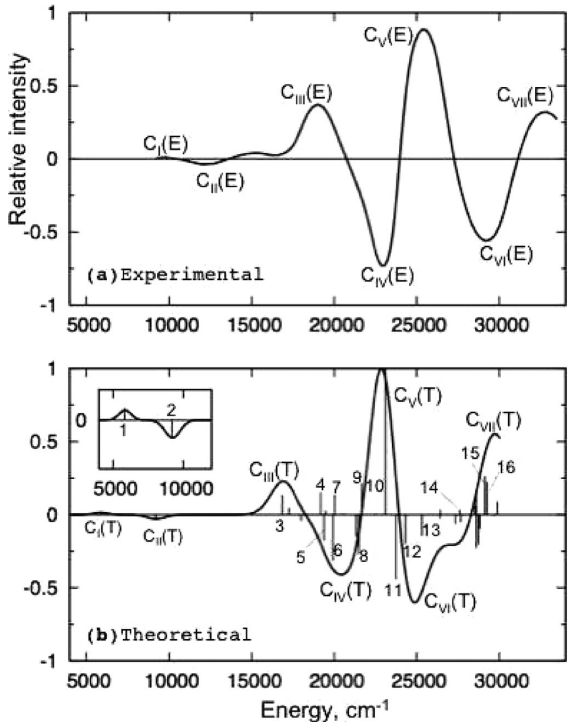

Figure 9. (a) Experimental (in poly(dimethylsiloxane) at 5 K and 7 T),[47] and (b) theoretical MCD spectra for [(Tp*)MoO(bdt)].

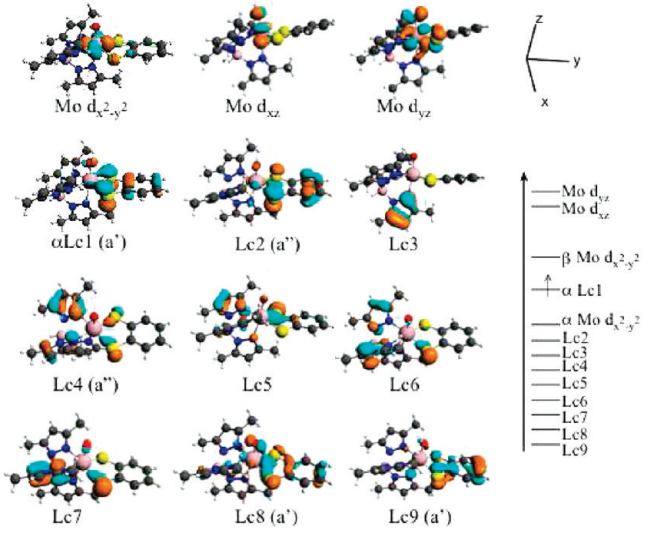

Figure 10. Plots of the molecular orbitals involved in the main transitions that give rise to the calculated electronic excitations for [(Tp*)-MoO(bdt)]. A qualitative orbital energy level diagram is also shown.

Next, as in the case of [(Tp*)MoO(bdt)], the excitation around 20000 cm^{-1} (excitation 5), is the first d-d transition with a Mo $d_{xy} \rightarrow$Mo d_{xz} assignment. Following excitation 5, according to Table 7, between 21100 and 23320 cm^{-1} we find some excitations (6 to 9) that include LMCT transitions from the Ld2 and Ld1 orbitals to Mo d_{xz} and Mo d_{yz}. Judging from the intensities of those excitations, the "out-of-plane" Ld2 orbital (with major contributions from the S p_z orbitals on the dithiolate ligand) interact poorly with the Mo d_{xz} orbital. Because excitations 11 and 13 are also very weak (Figure 11b), there is also a poor overlap between the orbital Ld2 and the orbitals Mo d_{yz}

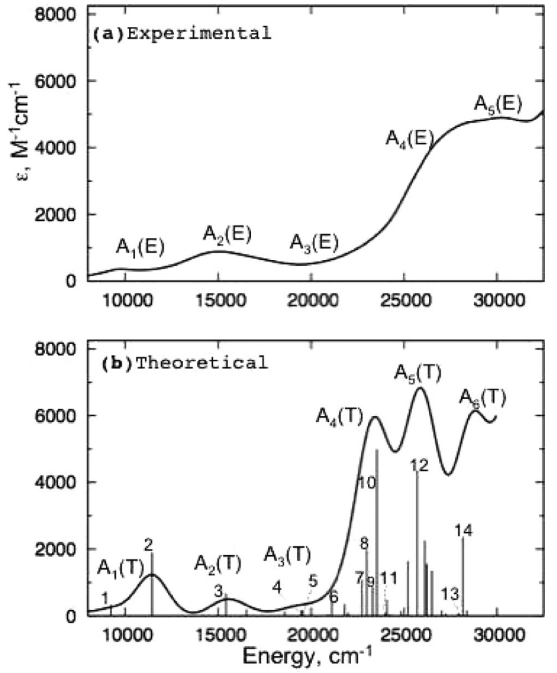

Figure 11. (a) Experimental (in 1,2-dichloroethane solution at room temperature)[47] and (b) theoretical absorption spectra for [(L3S)MoO-(bdt)].

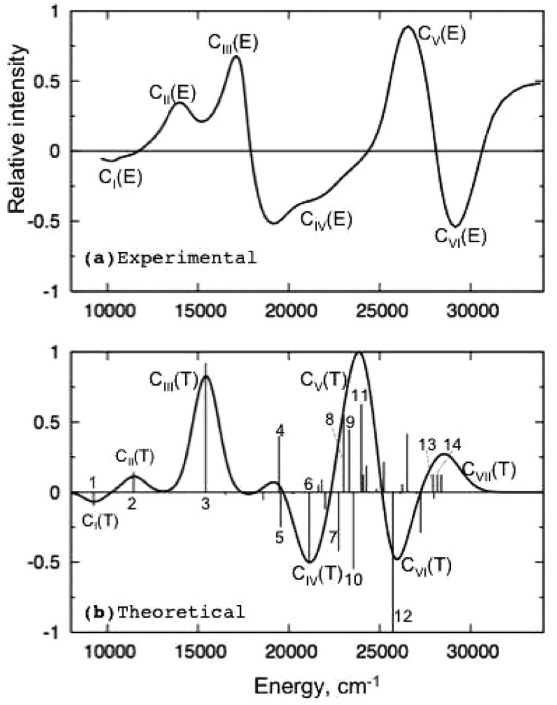

Figure 12. (a) Experimental (in poly(dimethylsiloxane) at 5 K and 7 T),[47] and (b) theoretical MCD spectra for [(L3S)MoO(bdt)].

and d_{xz}+Np_y, respectively. The most intense excitation (10) is calculated at 23560 cm^{-1} and its main contribution comes from the Ld1 $\rightarrow$ d_{xz}+Np_y transition. The orbital d_{xz}+Np_y is shown in Figure 13, and we see a π antibonding interaction of the p_y orbital from the nitrogen of the equatorial pyrazolyl ring with the d_{xz} molybdenum orbital. In contrast to the weak excitation 11, excitation 12 is very intense, and although the biggest contribution is from the α-spin Ld2 $\rightarrow$ Mo d_{yz} transition, Table 7 reveals

Table 7. Theoretical Excitation Energies, Oscillator Strength (f), and Assignment of Excitations in Terms of Selected One-Electron Transitions for the Complex [(L3S)MoO(bdt)]

band $A_n(T)$	excitation	excitation energy [a]	transition [b]	% [c]	f
A1	1	9420	β Ld2 →Mo d_{xy}	98.5	0.0018
	2	11440	β Ld3 →Mo d_{xy}	97.8	0.0098
A2	3	15410	β Ld4 →Mo d_{xy}	99.2	0.0034
A3	4	19460	α Ld1 →Mo d_{yz}	77.0	0.0009
	5	19550	α Mo d_{xy} →Mo d_{xz}	73.3	0.0009
A4	6	21120	α Ld2 →Mo d_{xz}	61.4	0.0022
	7	22740	β Ld2 →Mo d_{xz}	42.4	0.0055
	8	23010	α Ld1 →d_{xz}+Np_y	35.7	0.0102
	9	23320	β Ld3 →Mo d_{xz}	49.2	0.0044
	10	23560	α Ld1 →d_{xz}+Np_y	40.6	0.0258
	11	23990	α Ld2 →Mo d_{yz}	65.6	0.0005
A5	12	25720	β Ld2 →Mo d_{yz}	29.9	0.0073
			α Ld3 →Mo d_{yz}	25.3	
A6	13	27920	α Ld2 →d_{xz}+Np_y	46.7	0.0004
			β Ld2 →d_{xz}+Np_y	42.8	
	14	28170	β Ld3 →Mo d_{yz}	29.1	0.0122
			α Ld3 →Mo d_{yz}	26.8	

[a] Energies in cm^{-1}. [b] The orbitals are shown in Figure 13. [c] Percent contribution of the leading one-electron transition to the $A \rightarrow J$ excitation, where A represents the ground state.

that this contribution accounts only for 30% of the total composition of the excitation. A quantitatively similar contribution of 25% comes from the α Ld3 → Mo d_{yz} transition, where the Ld3 orbital contains an interaction with the S p_z from the thiolate ligand. Finally, an excitation of medium intensity at 28170 cm^{-1} is also an Ld3 → Mo d_{yz} transition. Thus, the S p_z thiolate orbital overlaps more efficiently with the Mo d_{yz} orbital, compared to its S p_z dithiolate counterpart.

The good agreement between the experimental and calculated MCD spectra can be verified in Figure 12. According to the results in Table 8, the C-parameters that give rise to the three MCD bands between 9400 and 15500 cm^{-1} are all dominated by the contribution of the spin−orbit perturbation of the ground state, C_J^G. Experimentally, a very broad negative band, $C_{IV}(E)$, was measured around 20000 cm^{-1}. According to the calculated C-parameters, this negative MCD band arises from at least seven different excitations. The majority of those excitations give rise to negative C-parameters. However, at 19460 cm^{-1} (excitation 4) appears a positive C-parameter dominated by the C_J^E contribution. For C_4^E, the mixing of excitation 4 with excitation 5 is the main contribution to the term. Likewise, the mixing of excitation 4 with excitation 5 constitutes the principal contribution to the C_5^E term with the direct consequence of giving a negative parameter at 19550 cm^{-1}. A relatively intense negative parameter C_6 arises from the Ld2 →Mo d_{xz} transition. Next, the positive band $C_V(E)$ around 26000 cm^{-1} may be made up of several excitations. The simulated term $C_V(T)$ contains C-parameters, most of them positive, except C_7 and C_{10} (Figure 12b). The intensity of those negative parameters is not enough to overcome the more intense and positive parameters such as C_8, C_9, and C_{11}. The relative intensity of the parameter C_{12} calculated around 26000 cm^{-1} is enough to make a negative band, $C_{VI}(T)$, that also is measured experimentally around 29000 cm^{-1}. The C_{12} parameter arises from the combination of the Ld2 →Mo d_{yz} and Ld3 →Mo d_{yz} transitions. Finally, a positive band $C_{VII}(T)$ is calculated to arise from

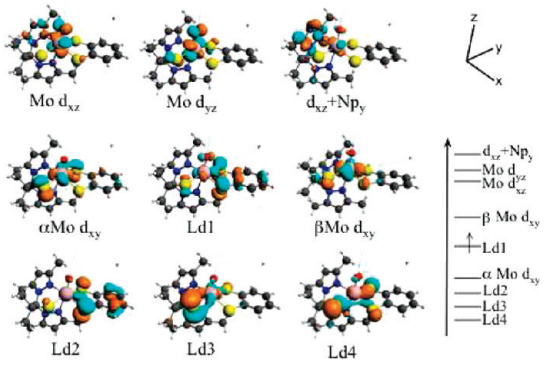

Figure 13. Plots of the molecular orbitals involved in the main transitions that give rise to the calculated electronic excitations for [(L3S)MoO(bdt)]. Also shown is a qualitative orbital energy level diagram.

Table 8. Principal C-Parameters[a] from the Complex [(L3S)MoO(bdt)]

C-term	J^b	C_J^c	C_J^{Gd}	C_J^{Ee}
C_I	1	−0.47	−0.51	0.04
C_{II}	2	0.67	0.79	−0.12
C_{III}	3	4.37	5.53	−1.16
C_{IV}	4	1.90	0.40	1.50
	5	−1.18	0.13	−1.31
	6	−2.36	−0.60	−1.76
	7	−2.00	0.47	−2.47
C_V	8	2.63	−0.39	3.02
	9	2.11	0.34	1.77
	10	−2.59	−0.25	−2.34
	11	2.98	−0.31	3.29
C_{VI}	12	−4.72	−1.35	−3.37
C_{VII}	13	0.61	0.05	0.56
	14	0.60	−0.54	1.14

[a] Values in au × 10^{-3}. [b] See Table 1 for details on the excitations. [c] Total value of the C-parameter of excitation J. [d] Contribution due to the spin−orbit coupling perturbation of the ground state, eq 5. [e] Contribution from the perturbation of the excited state J, eq 6; for details, see eq 4.

the Ld2 → d_{xz}-Np_y and Ld3 →Mo d_{yz} transitions, excitations 13 and 14, respectively.

Influence of the Ligands. Figure 14 displays the influence of the thiolate ligands on the ligand field splitting with respect to the effect of the chlorides. This figure shows the α- and β -spin orbital energy level diagram for all the systems under study. As a consequence of the relatively low energy of the chlorine orbitals, the first excitations (around 13000 cm^{-1}) are d-d transitions in the case of $[MoOCl_4]^-$. However, when the chlorides are substituted by thiolates with orbitals of higher energy, the transitions that occur at lower energies (9000 cm^{-1}) are evidently LMCT in nature. In fact, for [(Tp*)MoO(bdt)] and [L3SMoO(bdt)], the d-d transitions are calculated to appear even at higher energies with respect to the chloride complex, around 20000 cm^{-1}. The excitations of [L3SMoO(bdt)] appear at slightly higher energies when compared to the [(Tp*)MoO(bdt)] system. This can be explained by observing that the Mo−O distance is shorter in the former complex than in [(Tp*)MoO(bdt)] (1.66 vs 1.68 Å, respectively).[47] The consequence is a destabilization of the π^* Mo d_{xz} and Mo d_{yz} orbitals as shown in Figure 14, thus increasing the excitation energies on the [L3SMoO(bdt)] complex. The MCD spectra of the [(Tp*)MoO(bdt)] and [L3SMoO(bdt)] appear to be similar, especially at higher energies, for the positive C-term at ~25000 cm^{-1}. In both instances, the C-term originates

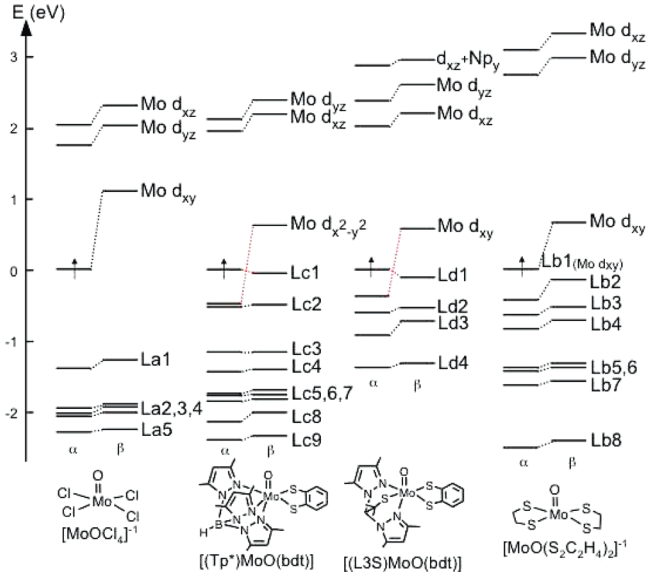

Figure 14. Orbital energy level diagrams for the systems under study. All the orbital energies have been referenced to the α-spin HOMO of each molybdenyl complex.

from an "out-of-plane" a″ S dithiolate LMCT (see excitation 10 in Table 5 and orbital Lc2 in Figure 10, and excitation 11 in Table 6 and orbital Ld2 in Figure 13). However, the negative C-term around 29000 cm^{-1} for [(Tp*)MoO(bdt)] arises from several excitations, one of them an "out-of-plane" a′ S dithiolate LMCT (excitation 12, Table 5) and another is a LMCT from a ligand with major contributions from the pyrazolyl ring. On the other hand, for [(L3S)MoO(bdt)] the C-term arises mainly from an excitation that contains contributions from the thiolate ligand (see excitation 12, Table 7). This shows that the presence of an additional thiolate ligand effectively influences the electronic structure of a complex with a dithiolate ligand bound to the metal center.

Concluding Remarks

We have presented the TD-DFT calculation of the electronic excitation and MCD parameters for a series of molybdenyl complexes. The qualitative agreement of the theoretical spectra with the experimental ones appears to be in general good. Compared to the $[MoOCl_4]^-$ complex, it was shown how the dithiolate/thiolate ligands induce LMCT transitions at low energies, while increasing the ligand field splitting so that the d-d transitions appear around values of up to 20000 cm^{-1}. In contrast, for example, it was previously stated that the first d-d transition in [(Tp*)MoO(bdt)] should appear around 15800 cm^{-1}.[48] In line with previous findings,[42,47−49] our calculations also indicate that the LMCT transitions originate from molecular orbitals mainly made up of "in-plane" and "out-of-plane" combinations of S p-orbitals at the dithiolate/thiolate ligands. From the results of our calculations, we have now proposed more detailed assignments for the excitations of [(L3S)MoO(bdt)]. Previously, some of the excitations only at low energies were tentatively assigned.[47] Likewise, new assignments have been proposed for the $[MoO(S_2C_2H_4)_2]^-$ absorption spectra. Previous work made use of an idealized C_{2v} model and of the Slater transition state formalism[43] to estimate the transition energies.[42] For example, the transitions $b_1(\sigma) \rightarrow$Mo d_{xy} and $b2(\sigma) \rightarrow$Mo d_{xy} were calculated to have the same excitation energy, allowing the assignment of the experimental excitation at 15900 cm^{-1} as a transition from the $b_2(\sigma)$ to the Mo d_{xy} orbitals.[42] However, we calculated the same transitions to appear around 19300 and 21200 cm^{-1}, respectively. Therefore we propose that the experimental excitation at 15900 cm^{-1} may correspond to a $b_2(\pi) \rightarrow$Mo d_{xy} transition, while the experimental excitation that appears at 18900 cm^{-1} may be attributed to a $b_1(\sigma) \rightarrow$Mo d_{xy} transition.

With respect to the theoretical calculations of the MCD spectra, it was found that most of the C-parameters that make up the MCD spectra are dominated by the mixing of the excited states (C_j^E). More importantly, the recent implementation into the ADF program of the methodology based on TD-DFT that includes the effect of spin−orbit coupling for the calculation of MCD parameters for paramagnetic systems[47] has proved to be a valuable tool in the simulation of MCD spectra showing a good agreement with the experimental results. Likewise, the recent modifications made to the methodology that allows for orbital degeneracies to be present, has given promising results for the correct simulation of the MCD C-terms in the symmetrized C_{4v} structure of $[MoOCl_4]^-$.

Acknowledgment. This work was supported by NSERC. T.Z. would like to thank the Canadian government for a Canada Research Chair. All calculations were performed using the Western Canada Research Grid computing resources (www.westgrid.ca).

(49) McNaughton, R. L.; Helton, M. E.; Rubie, N. D.; Kirk, M. L. *Inorg. Chem.* **2000**, *39*, 4386.